Available online at www.sciencedirect.com
SCIENCE DIRECT
Geochimica et Cosmochimica Acta 70 (2006) 1548–1564
Geochimica
www.elsevier.com/locate/gca

Origin of SiO_2-rich components in ordinary chondrites

Dominik C. Hezel [a,*], Herbert Palme [a], Lutz Nasdala [b], Frank E. Brenker [a]

[a] Universität zu Köln, Institut für Geologie und Mineralogie, Zülpicherstr. 49b, D-50674 Köln, Germany
[b] Johannes-Gutenberg Universität Mainz, Institut für Geowissenschaften-Mineralogie, Becherweg 21, D-55099 Mainz, Germany

Received 31 January 2005; accepted in revised form 22 November 2005

Abstract

Silica-rich objects are common minor components in ordinary chondrites (OC), occurring as fragments and as chondrules. Their typical paragenesis is orthopyroxene + SiO_2 (with bulk SiO_2 >65 wt%) and occasionally with additional olivine and/or spinel. Individual silica-rich components (SRC) have previously been studied in various types of OCs, although there is only one comprehensive study of these objects by Brigham et al. [Brigham, C.A., Murrell, M.T., Yabuki, H., Ouyang, Z., El Goresy, A., 1986. Silica-bearing chondrules and clasts in ordinary chondrites. Geochim. Cosmochim. Acta 50, 1655–1666]. Several different explanations of how SRCs formed have been published. The main question is how silica-enrichment was achieved, because CI-chondritic atomic Mg/Si-ratio is 1.07 and as a consequence only olivine and pyroxene, but no free silica should be stable. There are two basic possibilities for the SiO_2-enrichment: (1) a RedOx-mechanism or magmatic fractionation on the parent body and (2) fractional condensation or recycling of chondrule mesostasis in the solar nebula. To better constrain the origin of these objects, we measured major and rare earth elements in SRCs of various types of ordinary chondrites, and in addition, we studied silica polymorphism in these objects using an in situ micro-Raman technique. Bulk chondrule compositions define mixing lines between the compositions of olivine and pyroxene. The SRCs extend these lines to an SiO_2 end member. In contrast, magmatic trends grossly deviate from these mixing lines. Concentrations of CaO, Al_2O_3, and REE in the pyroxenes of the SRCs are low (0.01 to 1× CI) and the CI-normalized REE-patterns are virtually flat, typical of bulk chondrules, but untypical of magmatic trends. We therefore conclude that SiO_2-rich objects are not of magmatic origin. They are the result of fractional condensation in the solar nebula. The silica in SRCs occurs mainly as tridymite and sometimes as cristobalite or—in very rare cases—as quartz. Some SiO_2-phases yielded a yet unknown micro-Raman spectrum, which we were unable to identify. The often chondrule-like shape of SRCs as well as the presence of high-temperature SiO_2-polymorphs lead to the following model for the origin of SRCs: formation of SiO_2-rich precursors in the solar nebula by fractional condensation, reheating to temperatures between 1140 and >1968 K, thereby forming the SRCs,—probably during the chondrule-forming process—followed by rapid cooling.

1. Introduction

SiO_2-rich components (SRC) generally consist of orthopyroxene and a silica-polymorph, with a bulk SiO_2-content exceeding 65 wt% in most cases (Hezel et al., 2003). Few SRCs contain olivine and spinel. SRCs are rare but widespread objects in all main groups (H, L, and LL) and petrologic types of ordinary chondrites (OC), occurring in about 40% of these meteorites. The modal abundance of SRCs usually does not exceed ~1 vol % and sometimes only a single object is observed in a thin section. Some meteorites contain a large number of SRCs, for example, DaG 327 (H3), Devgaon (H3.8), and Seres (H4). The mineralogy of SRCs is quite diverse. In decreasing order of occurrence, reported mineral assemblages are: (1) SiO_2-pyroxene (e.g., Binns, 1967; Olsen et al., 1981; Planner, 1983; Brigham et al., 1986; Bridges et al., 1995; Kring et al., 2000; Murty et al., 2004), (2) SiO_2-pyroxene-fayalite (Brigham et al., 1986), (3) SiO_2-fayalite (Brigham et al., 1986; Wasson and Krot, 1994; Newton et al., 1995), (4) SiO_2-pyroxene-feldspar (Bridges et al., 1995; Ruzicka et al., 1995), (5) SiO_2-merrihueite/roedderite (Krot and Wasson, 1994), (6) SiO_2-K-feldspar-albite-Cl-apatite-whitlockite-ilmenite-zircon-pyroxene-Na, Ti-bearing silicate (Bischoff et al., 1993), (7) SiO_2-metal (Lauretta and Buseck, 2003; see Table 1).

* Corresponding author.
E-mail address: d.hezel@uni-koeln.de (D.C. Hezel).

0016-7037/$ - see front matter © 2005 Elsevier Inc. All rights reserved.
doi:10.1016/j.gca.2005.11.026

Table 1
Reports of free silica in ordinary chondrites

Meteorite	Type	SiO_2-polymorph	Reference
Bremervörde	H3	crs (*a*)	Brigham et al. (1986)
Sharps	H3.4	—	Brigham et al. (1986), Wasson and Krot (1994)
Devgaon	H3.8	—	Murty et al. (2004)
Dhajala	H3-4	—	Brigham et al. (1986)
Seres	H3-4	—	Brigham et al. (1986)
Elm Creek	H4	—	Wasson and Krot (1994)
Orique	H4	—	Kring et al. (2000)
Jilin	H4-5?	crs (*x*)	Brigham et al. (1986)
Morro do Rocio	H5	trd (*m*)	Wlotzka and Fredriksson (1980), Fredriksson and Wlotzka (1985), Brigham et al. (1986)
ALHA77011	L/LL3.5	—	Krot and Wasson (1994)
ALHA77015	L3	—	Fujimaki et al. (1981), Brigham et al. (1986)
Mezö-Madaras	L3	crs (*s*)	Dodd et al. (1965), Dodd et al. (1966), Brigham et al. (1986), Wood and Holmberg (1994), Krot and
Bovedy	L3	trd (*f*&*s*)	Ruzicka and Boynton (1992), Ruzicka et al. (1993), Ruzicka et al. (1995)
Krymka	L3.1	—	Wasson and Krot (1994)
ALHA77170	L3.6	—	Wasson and Krot (1994)
ALHA77115	L3.6	—	Wasson and Krot (1994), Krot and Wasson (1994)
Saratov	L4	—	Brigham et al. (1986)
Farmington	L5	crs (*x*)	Binns (1967), Brandstätter and Kurat (1985), Brigham et al. (1986), Bridges et al. (1995)
Knyahinya	L5	—	Brandstätter and Kurat (1985)
Nadiabondi	L6	crs (*x*)	Christophe-Michel-Levy and Curien (1965), Brigham et al. (1986)
ALHA76003		crs (*x*)	Olsen et al. (1981), Brigham et al. (1986)
Lissa	L6	—	Brandstätter and Kurat (1985)
Bishunpur	LL3.1	—	Lauretta and Buseck (2003)
Piancaldoli	LL3	crs (*s*)	Planner (1983), Brigham et al. (1986)
Parnallee	LL3.6	trd, Crs (*x*)	Hamilton et al. (1979), Bridges et al. (1995)
Adzhi-Bogdo	LL3.6	qtz, trd (*m*)	Bischoff et al. (1993)
ALHA77278	LL3.7	—	Krot and Wasson (1994)

Identification of polymorphs: (*a*), polymorph assumed; (*x*), X-ray diffractometry; (*m*), microscopically; (*s*), shape of silica; (*f*&*s*), FeO-content of the silica and shape of silica; and "—", polymorph not determined.

The discussion about the origin of SRCs is an ongoing debate since the first and so far only comprehensive paper about these objects by Brigham et al. (1986). The primary problem is to explain their unusual high bulk SiO_2-contents that allow the presence of free silica. As pointed out by Brigham et al. (1986), the elemental composition of the average solar system includes approximately the same number of Mg, Si, and Fe atoms, indicating that the resulting mineralogy should be olivine and pyroxene normative—albeit the fact that Fe is to a large extent present as metal—and an SiO_2 phase would not be stable. Several mechanisms have been suggested to achieve SiO_2-oversaturation during SRC formation: (i) Fractional condensation, which leads to SiO_2-condensation at temperatures around 1215 K and $P = 10$ Pa (e.g., Brigham et al., 1986; Petaev and Wood, 1998; Krot et al., 2004) due to incomplete reaction of earlier condensed solids—primarily forsterite—with the cooling nebula. (ii) Fractional crystallization of a melt on a parent body (e.g., Bridges et al., 1995; Ruzicka et al., 1995). (iii) Extreme reduction of chondritic olivine and pyroxene (e.g., Brigham et al., 1986). (iv) Sulfurization of pyroxene, as proposed by Rubin (1983) for the formation of SiO_2 in enstatite chondrites. (v) Oxidation of Si-rich metals (Brandstätter and Kurat, 1985).

SiO_2 has three main and several sub-polymorphs at a pressure of 10^5 Pa. These are: quartz, tridymite, and cristobalite. In addition, there is SiO_2-glass. Identification of the polymorph present in a mineral assemblage helps to understand the temperature history of silica-bearing objects. A systematic study of SiO_2-polymorphs in meteorites does not exist, occasional reports of SiO_2-polymorphs are from papers with a different focus. Table 1 is a comprehensive listing of SiO_2-polymorphs found in OCs along with the method that was used to identify these polymorphs.

In this study, we present concentrations of major and rare earth elements in SRCs and we include for the first time in situ studies of SiO_2-polymorphs in SRCs of OCs. Based on these data various possibilities of SiO_2-enrichment are discussed. Preliminary results were published in Hezel et al. (2004a,b).

2. Methods

We performed detailed petrographic and petrologic studies of SRCs in 24 thin sections of 19 different OCs (Table 2). Mineral analyses were made with a JEOL 8900RL electron microprobe (EMP). The accelerating voltage was set to 15 kV and the beam current to 20 nA. The ZAF-algorithm was used for correction. Back scattered electron (BSE) images were taken with the same EMP. Bulk SRC compositions of individual elements were calculated using the simple formula (conc., element concentration):

Table 2
Occurrence of silica-polymorphs in different types of ordinary chondrites measured in this study

Meteorite	Type	Samples[a]	Quartz	Tridymite	Cristobalite	Glass	Unknown[b]	Reported
Y193708	H3	1	—	—	—	—	—	No
DaG 327	H3	1	—	Yes	Yes	—	Yes	No
DaG 405	H3.5	1	—	—	Yes	—	—	No
Devgaon	H3.8	2	—	Yes	Yes	—	Yes	Yes
Dhajala	H3-4	1	—	—	—	—	—	Yes
Seres	H4	3	Yes	Yes	Yes	—	Yes	Yes
Kalaba	H4	1	—	—	—	—	—	Yes
Mezö-Madaras	L3	1	—	—	—	—	—	Yes
Bovedy	L3	1	Yes	—	—	—	Yes	Yes
Saratov	L4	1	—	—	—	—	—	Yes
Farmington	L5	2	—	—	Yes	—	—	Yes
Knyahinya	L5	2	—	Yes	—	—	Yes	Yes
Lissa	L6	1	—	—	—	—	Yes	Yes
DaG 369	H/L3	1	—	—	—	—	—	No
DaG 378	H/L3	1	—	—	—	—	—	No
Semarkona	LL3.0	1	—	—	—	—	—	No
Bishunpur	LL3.1	1	—	—	—	—	—	No
Parnallee	LL3.6	1	Yes	Yes	Yes	—	Yes	Yes
Krähenberg	LL5	1	—	—	—	—	—	No

[a] Number of thin sections investigated in this study.
[b] Polymorphs with unknown Raman spectra (see text).

$$\text{element}_1 = \sum(\text{area}_{\text{phase }1} \cdot \text{conc. in phase } 1) + \ldots + (\text{area}_{\text{phase }n} \cdot \text{conc. in phase } n).$$

The area of a phase was measured from BSE-images using image processing software. The concentrations of elements in a certain phase were determined from EMP analyses. We are aware of the problems of determining element abundances in a 3-dimensional object by analyzing a 2-dimensional section arbitrarily crosscutting the object. However, considering the simple mineralogy of these objects and the seemingly homogeneous distribution of silica and pyroxene, uncertainties in the bulk analyses should be minimal.

The concentrations of rare earth elements (REE) were measured with the Cameca 3f ion microprobe at the Max-Planck-Institute für Chemie in Mainz. Oxygen was used as primary ions with a beam current of 10 nA, an acceleration voltage of 4.5 kV and 80 V offset. Spot size was 25 μm. Each mass was measured 30 s and the whole cycle was repeated six times. The calculated detection limit is in most cases between 2 and 10 ppb, depending on the element and the individual run. In rare cases, the detection limit reaches ~15 ppb. To account for possible fluctuations in the machine setting during a run, we assume a detection limit of 15 ppb for all REE.

Silica-polymorphs were studied using Raman microprobe analysis. The measurements were done by means of a Jobin Yvon (Horiba) LabRam HR800 system. This notch filter-based spectrometer was equipped with an Olympus BX41 microscope, a grating with 1800 grooves per mm and a Si-based charge-coupled device (CCD) detector. Spectra were excited with the He–Ne 632.8 nm emission (3 mW). With the Olympus 100× objective, the lateral resolution was better than 1.5 μm. The wave number accuracy was 0.5 cm^{-1} and the spectral resolution was 0.5 cm^{-1}.

MELTS calculations were done using the program of Ghiorso and Sack (1995). The starting composition was a metal free H-chondrite (data taken from Mason, 1965; SiO_2: 47.8, TiO_2: 0.20, Al_2O_3: 3.50, Cr_2O_3: 0.55, FeO: 12.7, MnO: 0.33, MgO: 31.0, CaO: 2.32, and Na_2O: 1.13; all data in wt%). This composition was chosen to compare our results with the calculations of Bridges et al. (1995), who also used H-chondrites as starting composition. We also calculated a magmatic trend using an L-chondrite as initial composition. The results of both calculations are very similar. We calculated trends with and without removal of solids from equilibrium and found that the differences are negligible. All calculations began at 1700 °C and the pressure was kept constant at 1 bar. It was not possible to reach the desired low temperature limit using the MELTS program. By slightly modifying the concentrations of five elements, we could extend the calculations to lower temperatures (between 1000 and 1100 °C) and therefore higher SiO_2-contents in the residual melt. The following changes were made (in wt%): SiO_2: 47.95, Al_2O_3: 3.51, Fe_2O_3: 0.02, FeO: 12.71, MgO: 31.1, and CaO: 2.33. Fe_2O_3 was included as required by the code. The calculated trend, thus, represents the evolution of a melt resulting from fractional crystallization (see Fig. 4).

All mineral abbreviations used follow the suggestions of Kretz (1983). Mineral abbreviations not listed in Kretz (1983) are explained in the text.

3. Results

We considered two aspects for selecting samples: (1) all main groups (H, L, and LL) and all petrologic types of OCs should be represented and (2) samples should be rich

in SRCs. We selected meteorites in which SiO_2-phases were previously reported and attempted to obtain from the authors the samples in which the SiO_2-rich objects were described. We also searched for SRCs in meteorites in which they have not been described before. We found SRCs in 9 of the 19 different OCs analyzed. In 10 meteorites, we found no SRCs, although previous reports indicated their presence.

3.1. Petrography

It was reported earlier that SiO_2-rich objects occur either as chondrules or as fragments (e.g., Brigham et al., 1986). The size of the fragments can vary considerably, up to 1.6 cm in diameter (Bridges et al., 1995). The majority of SRCs and all of the chondrule-like objects do not exceed the size of average chondrules in a meteorite. The appearances of SRCs are quite different, even in a single thin section. Fig. 1 emphasizes this variety. The SRCs can be broadly subdivided into four groups, according to their parageneses.

3.1.1. SRCs with pyroxene-SiO_2 (Figs. 1a–h)

The first three photomicrographs in the upper row of Fig. 1 show SRCs from the H3 DaG 327 meteorite. The first object (panel a) is a perfectly rounded chondrule with mostly pyroxene. SiO_2 is predominantly at the border and in one case small traces of mesostasis are between pyroxene grains. In the second object (panel b), a somewhat elongated chondrule, pyroxene is again dominant and the SiO_2 phase is predominantly at the rim. The third object (panel c) is a chondrule with less SiO_2 than the first two objects. The average size of the SRCs in DaG 327 is between 600–700 μm. This is at the upper end of chondrule diameters in this meteorite, ranging from ~200–600 μm. The next two objects (panels d and e) were the only SRCs found in a single section of the Bovedy L3 chondrite. The first (panel d) is clearly a fragment and the second a chondrule. Both SRCs are different from the Bo-1 clast in Bovedy described by Ruzicka et al. (1995). This clast is much larger at 4.5×7 mm and it contains feldspar. The two objects shown here contain mainly pyroxene, SiO_2, and traces of metal and have a typical L-chondrite chondrule size of 600–700 μm. The next three pictures (panels f–h) show SRCs from Devgaon (H3.8). This meteorite—like DaG 327 and Seres—contains many SRCs, but their individual appearances are all different. The first fragment (panel f) shows a perfect liquid immiscibility texture between SiO_2 and pyroxene, as described earlier in some objects of the CH-chondrite Acfer 182 by Hezel et al. (2003). Texturally it resembles the SRC in picture (panel l). Other SRCs in Devgaon also show immiscibility textures, although less pronounced. The more typical appearance of SRCs in Devgaon can be seen in the following two pictures (panels g and h): The first (panel g) is a chondrule with bleb-like SiO_2 intergrown with laths of pyroxene. The second (panel h) is a chondrule with skeletal SiO_2 within the pyroxene crystals. The average size of the SiO_2-objects is ~300 μm, about the average chondrule size of H-chondrites (Brearley and Jones, 1998 and references therein), but they may be as large as 600 μm. Although different in appearance, all SRCs in Devgaon have the same paragenesis: SiO_2-pyroxene.

3.1.2. SRCs with pyroxene-SiO_2, ±olivine, ±spinel (Figs. 1i–m)

These figures display objects from the Seres H4 meteorite, a meteorite comparatively rich in SRCs. The usual texture and paragenesis is, SiO_2 in the core, surrounded by pyroxene and a thin layer of olivine in the outer part. Their sizes range between 300 and 700 μm. This is high for H-chondrites, but chondrules in Seres are often about the same size. Some objects contain spinel (panel k) and in one case, few tiny metal grains (panel l) were encountered. As the Seres meteorite is metamorphosed, it is often difficult to decide if SRCs are chondrules or fragments. However, it is clear that the four SRCs (panels i–k, m) have rounded outlines and should be considered chondrules. The fifth object in Fig. 1l is a fragment. This SRC is also texturally different: the SiO_2 phases are rounded, typical of immiscible liquids and thus resembling SRCs from Devgaon (Fig. 1f) or CH-chondrites (Hezel et al., 2003). The chondrule-like SRC in panel m is also slightly different from most Seres SRCs in having no olivine rim and SiO_2-laths are scattered throughout the whole SRC.

3.1.3. A single unique SRC with olivine-SiO_2 (Fig. 1n)

Photomicrograph (panel n) shows a unique object in the H3.5 DaG 405 chondrite. It has a large diameter of ~700 μm compared to chondrules in this thin section, which range in size from ~300 to 600 μm, however, there are also many smaller as well as some larger objects. In panel n, skeletal SiO_2-crystals are embedded in a fine-grained matrix of SiO_2 intergrown with olivine. The olivine was identified using micro-Raman as it was not possible to identify the fine-grained olivine with the EMP. The whole object has a two layer structure (highlighted by the dashed line) with core and rim, but both have similar textures.

3.1.4. Others (Fig. 1o)

Bridges et al. (1995) described eight clasts in the Parnallee meteorite with the paragenesis pyroxene-SiO_2. One of the clasts contains abundant feldspar (Fig. 1o), intergrown with pyroxene and silica.

In summary, all objects analyzed here appear as chondrules or fragments with the typical paragenesis of SiO_2-pyroxene, sometimes with olivine, ±spinel, and ±metal. Exceptions are the olivine-rich object in panel n and a single plagioclase-bearing clast of the Parnallee meteorite (panel o; Bridges et al., 1995).

3.2. Chemical composition

3.2.1. SRCs with pyroxene-SiO_2 (Figs. 1a–h)

The SRCs shown in Fig. 1 contain virtually no mesostasis. The only abundant minerals are pyroxene and a

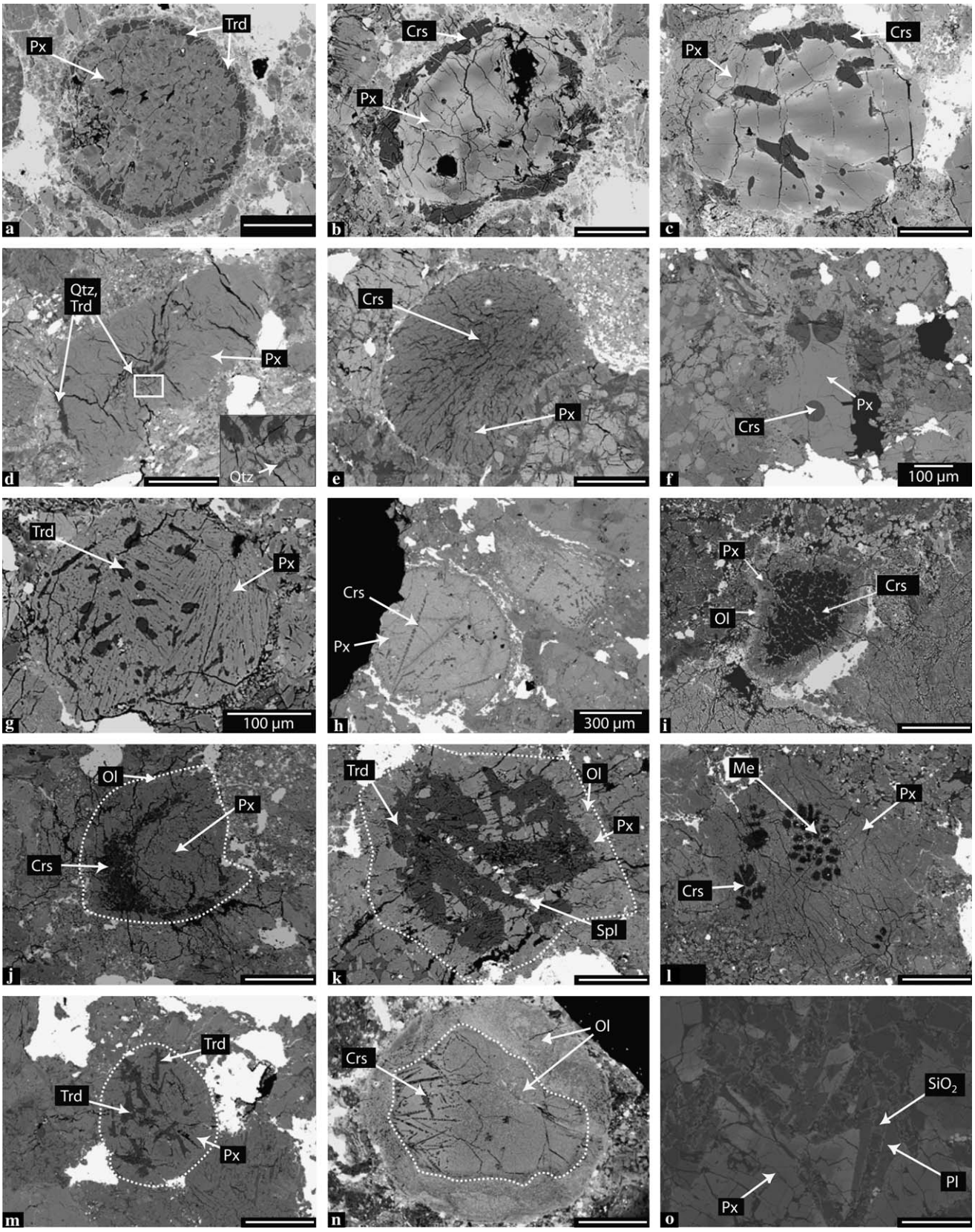

Fig. 1. BSE-images demonstrating variable appearances of SRCs. The most common type has the paragenesis pyroxene-SiO_2. (a–c) DaG 327 with pyroxene-SiO_2 paragenesis. Pyroxenes in (a) are zoned with decreasing MgO-concentrations from core (darker) to rim (brighter). Pyroxenes in (b) and (c) have domains with variable amounts of FeO. Brighter domains correspond with higher and darker with lower FeO-concentrations. (d–e) Bovedy with pyroxene-SiO_2 paragenesis. (f–h) Devgaon with pyroxene-SiO_2 paragenesis. (i–m) Seres with pyroxene-SiO_2, ±olivine, ±spinel paragenesis. (n) DaG 405 with olivine-SiO_2 paragenesis (o) Parnallee with pyroxene-SiO_2, ±feldspar paragenesis. If not labelled, scale bar is 200 µm. Px, pyroxene; Trd, tridymite; Crs, cristobalite; Qtz, quartz; Ol, olivine; Spl, spinel; and Me, metal.

silica-polymorph. The pyroxenes are mainly orthopyroxenes. Most of them are members of the solid solution series En–Fs with CaO-concentrations mostly below 1 wt%. The contents of other minor elements are also below 1 wt% (Table 3). The pyroxenes have variable amounts of FeO. Some SRCs in DaG 327 have zoned pyroxenes, with decreasing MgO-concentrations from core to rim (panel a). In other SRCs, individual pyroxene grains cannot be identified, but apparently there are MgO- and FeO-rich domains (panels b and c). The lowest and highest FeO-concentrations, respectively, found in these pyroxenes are given in Table 3. In Devgaon, FeO-concentrations in SRC-pyroxenes are highly variable. The SiO_2 phase is usually very pure, sometimes with traces of FeO of up to 0.52 wt%.

Rare earth elements are very low in all pyroxenes analyzed and most of the REE-patterns are unfractionated (Fig. 2). Abundances are between 0.1 and 1 times CI-chondritic and CI-normalized La/Yb-ratios range from 0.16 to 2.44 in Devgaon and from 0.51 to 0.81 times CI in Bovedy. Half of the pyroxenes in Devgaon and Bovedy have a negative, the other half a positive Eu-anomaly. The measure for the size of the Eu-anomaly is given as the Eu/Eu^*-ratio, which is the CI-normalized Eu-concentration, divided by the CI-normalized average concentration of Sm and Gd, the two neighboring elements to Eu (Table 4). In SiO_2 phases, REE are below detection limits. The modal content of pyroxenes in SRCs is at most ~50%. Thus the bulk REE-concentrations in SRCs should be at least a factor of two lower than those in pyroxenes, in most cases even more.

3.2.2. SRCs with pyroxene-SiO_2, ±olivine, ±spinel (Figs. 1i–m)

Most SRCs in the Seres meteorite contain olivine. The chemical composition of individual phases is the same in all SRCs from this meteorite. Olivines have $Fa_{18–19}$ and pyroxenes Fs_{18}. Manganese concentrations in olivine and pyroxene are around 0.5 wt%, which is at the upper limit of chondrule Mn-concentrations (e.g., Klöck et al., 1989). All other minor element contents are below 1 wt%. In one SRC (panel k), abundant chromite is present (Table 3). The concentrations of rare earth elements were only determined in pyroxenes; the contents in olivine and spinel are below detection limits. The absolute REE-concentrations are low (Table 4) and most CI-normalized patterns are essentially flat (Fig. 2) with La/Yb-ratios between 0.21 and 2.5 times the CI-ratio. A few REE-patterns are slightly fractionated, with LREE > HREE. Three-fourths of the Seres SRCs have a negative; one-fourth has a positive Eu-anomaly.

3.2.3. A single unique SRC with olivine-SiO_2 (Fig. 1n)

This object is a fine intergrowth of olivine and cristobalite. EMP data were obtained using a broad beam with 30 μm diameter, as crystals were too small for individual mineral analyses. The low totals reflect the slightly porous structure of the object and/or might be the result of broad beam analysis. The center of this object has a chemical composition that is more siliceous than that of the rim, MgO and CaO show the opposite trend (Table 3). All other elements are uniformly distributed. The high CaO-concentration, especially in the border, indicates that another phase beside olivine and SiO_2 must be present. The abundance of this unknown phase should be quite low, as it could not be observed in the micro-Raman-spectra that indicated the presence of cristobalite and olivine.

3.2.4. Others (Fig. 1o)

This clast was previously analyzed and described by Bridges et al. (1995). Pyroxenes occur as ortho- and clinopyroxenes and plagioclase is anorthite-rich with An_{76}. Silica contains traces of FeO (0.21 wt%).

3.3. SiO_2-polymorphism

In Table 1, we list the OCs in which free silica was reported in earlier studies. In some cases, authors have identified the SiO_2-polymorph. This is indicated in Table 1 along with the method that was applied for identification. Table 2 gives an overview of the SiO_2-polymorphs that were found in this study and Fig. 3 shows examples of typical micro-Raman spectra. For reference spectra, the reader is referred to Scott and Porto (1967); Etchepare et al. (1974) and (Nasdala et al. (2004); alpha-quartz), (Etchepare et al. (1978); cristobalite and tridymite), and (Sharma et al. (1981); SiO_2 glass). The dominant SiO_2 phases are tridymite, cristobalite, and at least one so far unknown silica-polymorph, based on the Raman spectrum (see Fig. 3). Hezel et al. (2003) obtained this type of silica spectrum in the CH-chondrite Acfer 182. Based on TEM results, Hezel et al. (2003) excluded several possible SiO_2-polymorphs. A recent TEM-study of the silica phase yielding the unknown spectrum (Hezel, 2003) provided evidence for at least one sub-polymorph of tridymite (this mineral has a total of eight sub-polymorphs; Withers et al., 1994; Pride and Dove, 1998). Further work to unambiguously identify the unknown SiO_2-phases is in progress. No clear-cut evidence for the occurrence of SiO_2 glass was found. Silica glass, however, may easily be overlooked in the presence of other silica-polymorphs due to its comparatively low intensity Raman spectrum. Small traces of quartz were found in Seres and Bovedy. However, the clast in Parnallee contains more quartz than tridymite and only traces of cristobalite.

4. Discussion

Fig. 4 is a plot of Mg/Si- vs. 1/Si-ratios of bulk chondrules, SRCs and other rocks. Linear correlations in this plot represent mixing lines. Bulk compositions of type I and type II chondrules (Dodd, 1978; Kimura and Yagi, 1980; Grossman and Wasson, 1983; Olsen, 1983; Sears et al., 1984; Rubin and Pernicka, 1989; Jones, 1990, 1994, 1996; McCoy et al., 1991; Matsunami et al., 1993; Bridges et al., 1995; Ruzicka et al., 1995; Huang et al., 1996;

Table 3
Chemical composition of SRCs from different ordinary chondrites analyzed in this study

	DaG 327, a					DaG 327, b			
	Px	Px	Meso	Trd	Bulk	Px	Px	Crs	Bulk
SiO_2	57.04	59.15	61.90	101.63	66.02	55.11	57.95	99.40	68.59
TiO_2	0.03	0.04	0.53	<.03	0.05	0.03	<.03	<.03	<.03
Al_2O_3	0.20	0.26	18.66	0.01	0.79	0.35	0.21	0.02	0.26
Cr_2O_3	0.15	0.37	0.16	<.04	0.16	0.43	0.57	<.04	0.41
FeO	11.37	3.02	0.99	0.26	8.17	20.01	8.28	0.52	11.08
MnO	0.37	0.09	0.05	<.03	0.23	0.41	0.10	<.03	0.21
MgO	31.36	36.87	4.82	<.04	25.18	24.28	34.25	<.04	20.47
CaO	0.33	0.27	7.39	0.03	0.50	0.56	0.37	<.02	0.42
Na_2O	<.08	0.09	5.97	<.08	0.24	0.09	<.08	<.08	<.08
Total	100.86	100.17	100.46	101.96	101.34	101.27	101.72	100.03	101.50
Si	1.994	2.003	2.758	0.998	—	2.000	1.982	0.997	—
Ti	0.001	0.001	0.018	—	—	0.001	—	—	—
Al	0.008	0.010	0.980	0.000	—	0.015	0.008	0.000	—
Cr	0.004	0.010	0.006	—	—	0.012	0.015	—	—
Fe	0.333	0.085	0.037	0.002	—	0.607	0.237	0.004	—
Mn	0.011	0.003	0.002	—	—	0.013	0.003	—	—
Mg	1.635	1.861	0.320	—	—	1.314	1.746	—	—
Ca	0.012	0.010	0.353	0.000	—	0.022	0.014	—	—
Na	—	0.006	0.515	—	—	0.006	—	—	—
Total	3.999	3.989	4.989	1.001	—	3.989	4.006	1.003	—

	DaG 327, c				Bovedy, d			Bovedy, e		
	Px	Px	Crs	Bulk	Px	Qtz, Trd	Bulk	Px	Crs	Bulk
SiO_2	55.88	57.93	100.44	65.21	56.25	101.13	60.73	56.89	100.57	65.63
TiO_2	<.03	0.05	<.03	0.03	0.14	<.03	0.12	0.04	<.03	0.04
Al_2O_3	0.23	0.44	0.04	0.37	0.92	0.11	0.84	0.34	0.22	0.31
Cr_2O_3	0.50	0.65	<.04	0.55	0.33	<.04	0.30	0.27	0.07	0.23
FeO	15.16	9.38	0.35	9.96	12.81	0.25	11.55	10.88	0.39	8.79
MnO	0.39	0.16	<.03	0.21	0.49	<.03	0.45	0.48	<.03	0.39
MgO	28.37	32.51	<.04	24.66	28.31	0.27	25.50	30.90	0.69	24.86
CaO	0.43	0.44	<.02	0.42	1.20	0.21	1.10	0.40	0.68	0.45
Na_2O	0.10	<.08	<.08	<.08	0.10	<.08	0.10	<.08	0.15	<.08
Total	101.05	101.57	100.87	101.45	100.55	102.05	100.70	100.24	102.82	100.76
Si	1.988	1.993	0.998	—	1.992	0.995	—	1.999	0.986	—
Ti	—	0.001	—	—	0.004	—	—	0.001	—	—
Al	0.010	0.018	0.000	—	0.038	0.001	—	0.014	0.003	—
Cr	0.014	0.018	—	—	0.009	—	—	0.008	0.001	—
Fe	0.451	0.270	0.003	—	0.379	0.002	—	0.320	0.003	—
Mn	0.012	0.005	—	—	0.015	—	—	0.014	—	—
Mg	1.505	1.667	—	—	1.494	0.004	—	1.618	0.010	—
Ca	0.016	0.016	—	—	0.046	0.002	—	0.015	0.007	—
Na	0.007	—	—	—	0.007	—	—	—	0.003	—
Total	4.003	3.989	1.002	—	3.984	1.005	—	3.990	1.013	—

	Devgaon, f			Devgaon, g			Devgaon, h		
	Px	Crs	Bulk	Px	Trd	Bulk	Px	Crs	Bulk
SiO_2	56.38	99.33	65.89	56.51	98.47	68.49	54.40	99.11	59.97
TiO_2	0.06	<.03	0.03	0.06	<.03	0.04	0.03	<.03	0.03
Al_2O_3	0.88	0.18	0.74	0.90	0.16	0.69	0.39	0.12	0.36
Cr_2O_3	0.31	<.04	0.31	0.47	0.04	0.35	0.66	<.04	0.58
FeO	9.94	0.33	7.71	8.26	0.24	5.98	18.41	0.41	16.16
MnO	0.54	<.03	0.44	0.50	<.03	0.36	0.69	0.03	0.60
MgO	29.91	0.31	23.33	31.73	0.32	22.79	23.99	<.04	21.00
CaO	0.71	0.07	0.62	0.84	0.24	0.67	1.08	<.02	0.95
Na_2O	0.26	<.08	0.22	0.24	0.12	0.21	0.26	<.08	0.24
Total	98.99	100.32	99.28	99.52	99.62	99.59	99.92	99.79	99.90
Si	2.000	0.994	—	1.982	0.993	—	1.996	0.996	—
Ti	0.002	—	—	0.001	—	—	0.001	—	—
Al	0.037	0.002	—	0.037	0.002	—	0.017	0.001	—

Table 3 (*continued*)

	Devgaon, f			Devgaon, g			Devgaon, h		
	Px	Crs	Bulk	Px	Trd	Bulk	Px	Crs	Bulk
Cr	0.009	—	—	0.013	0.000	—	0.019	—	—
Fe	0.295	0.003	—	0.242	0.002	—	0.565	0.003	—
Mn	0.016	—	—	0.015	—	—	0.021	0.000	—
Mg	1.582	0.005	—	1.659	0.005	—	1.313	—	—
Ca	0.027	0.001	—	0.032	0.003	—	0.043	—	—
Na	0.018	—	—	0.017	0.002	—	0.019	—	—
Total	3.985	1.006	—	3.999	1.007	—	3.994	1.003	—

	Seres, i				Seres, j			
	OI	Px	Crs	Bulk	OI	Px	Crs	Bulk
SiO_2	41.08	58.05	100.01	70.76	39.79	53.61	100.45	77.74
TiO_2	<.03	0.06	<.03	0.02	<.03	0.07	<.03	0.03
Al_2O_3	0.04	0.18	0.03	0.08	0.01	0.16	<.01	0.06
Cr_2O_3	<.04	0.16	<.04	0.06	0.04	0.24	<.04	0.10
FeO	14.74	9.60	0.17	7.07	14.41	9.95	0.24	5.07
MnO	0.55	0.53	<.03	0.33	0.52	0.46	<.03	0.22
MgO	42.87	29.48	0.50	21.10	44.86	30.94	0.06	15.41
CaO	0.04	0.98	0.08	0.39	0.05	4.25	<.02	1.64
Na_2O	<.08	<.08	<.08	<.08	<.08	0.20	<.08	0.08
Total	99.40	99.10	100.85	99.87	99.68	99.90	100.79	100.36
Si	1.033	2.046	0.995	—	1.001	1.920	0.998	—
Ti	—	0.001	—	—	—	0.002	—	—
Al	0.001	0.007	0.000	—	0.000	0.007	—	—
Cr	—	0.004	—	—	0.001	0.007	—	—
Fe	0.310	0.283	0.001	—	0.303	0.298	0.002	—
Mn	0.012	0.016	—	—	0.011	0.014	—	—
Mg	1.607	1.549	0.007	—	1.682	1.652	0.001	—
Ca	0.001	0.037	0.001	—	0.001	0.163	—	—
Na	—	—	—	—	—	0.014	—	—
Total	2.967	3.948	1.006	—	2.999	4.078	1.002	—

	Seres, k					Seres, l		
	Ol	Px	Spl	Trd	Bulk	Px	Crs	Bulk
SiO_2	37.96	55.19	0.18	100.57	69.49	58.24	100.00	65.34
TiO_2	<.03	<.03	0.31	<.03	<.03	0.08	<.03	0.06
Al_2O_3	0.03	0.14	11.26	0.03	0.24	0.73	0.22	0.65
Cr_2O_3	<.04	0.20	56.32	<.04	0.90	0.42	0.05	0.36
FeO	15.03	9.91	24.62	0.28	7.15	10.09	0.20	8.41
MnO	0.47	0.51	0.80	<.03	0.29	0.53	<.03	0.44
MgO	44.71	30.98	4.82	<.04	20.49	28.99	<.04	24.06
CaO	<.02	1.63	0.03	<.02	0.60	0.85	<.02	0.70
Na_2O	<.08	<.08	<.08	<.08	<.08	0.13	<.08	0.12
Total	98.29	98.64	98.34	100.96	99.23	100.07	100.57	100.15
Si	0.975	1.976	0.006	0.998	—	2.037	0.996	—
Ti	—	—	0.008	—	—	0.002	—	—
Al	0.001	0.006	0.458	0.000	—	0.030	0.003	—
Cr	—	0.006	1.536	—	—	0.012	0.000	—
Fe	0.323	0.297	0.710	0.002	—	0.295	0.002	—
Mn	0.010	0.015	0.023	—	—	0.016	—	—
Mg	1.713	1.654	0.248	—	—	1.512	—	—
Ca	—	0.062	0.001	—	—	0.032	—	—
Na	—	—	—	—	—	0.009	—	—
Total	3.025	4.020	2.989	1.002	—	3.945	1.003	—

	Seres, m			DaG 405, n			Parnallee, o		
	Px	Trd	Bulk	AV Border	AV Center	Bulk	CB8[a]	CB2[a]	CB3[a]
SiO_2	56.65	101.03	71.79	41.16	59.42	52.14	62.90	78.90	65.30
TiO_2	<.03	<.03	<.03	<.03	0.03	<.03	0.00	0.00	0.00
Al_2O_3	0.24	0.01	0.16	1.07	0.98	0.98	1.90	0.00	0.50

(*continued on next page*)

Table 3 (*continued*)

	Seres, m			DaG 405, n			Parnallee, o		
	Px	Trd	Bulk	AV Border	AV Center	Bulk	CB8[a]	CB2[a]	CB3[a]
Cr_2O_3	0.30	<.04	0.20	0.63	0.60	0.59	0.40	0.20	0.50
FeO	9.54	0.21	6.35	19.38	17.80	17.72	9.40	4.50	5.60
MnO	0.42	<.03	0.28	0.42	0.61	0.48	0.10	0.20	0.00
MgO	31.58	<.04	20.82	23.68	16.47	19.32	21.10	7.70	25.40
CaO	0.39	<.02	0.26	4.19	0.98	2.57	3.50	8.20	2.40
Na_2O	<.08	<.08	<.08	0.41	0.63	0.49	0.40	0.10	0.20
Total	99.16	101.31	99.88	90.98	97.54	94.32	99.70	99.80	99.90
Si	2.000	0.999	—	—	—	—	—	—	—
Ti	—	—	—	—	—	—	—	—	—
Al	0.010	0.000	—	—	—	—	—	—	—
Cr	0.008	—	—	—	—	—	—	—	—
Fe	0.282	0.002	—	—	—	—	—	—	—
Mn	0.013	—	—	—	—	—	—	—	—
Mg	1.662	—	—	—	—	—	—	—	—
Ca	0.015	—	—	—	—	—	—	—	—
Na	—	—	—	—	—	—	—	—	—
Total	3.991	1.001	—	—	—	—	—	—	—

All analyses are in wt%. The numbers of cations are given. Most analyses are single point analyses, except for Bovedy and Seres. These are mean values from a set of point analyses. The sums of the DaG 405 analyses are too low, possibly the result of broad beam analyses. Data given in the table correspond to the SRCs shown in Fig. 1; the letter after the meteorite name refers to the corresponding image in Fig. 1. Bulk compositions are calculated (see text). Meso, mesostasis; and AV, average.

[a] Analysis taken from Bridges et al. (1995).

Tachibana et al., 2003; Hezel et al., 2004a) fall along mixing lines between olivine and SiO_2. Variable amounts of FeO in the mafic minerals and some variations in Al_2O_3 + CaO-contents of the mesostases lead to deviations from the Fo–SiO_2 line. Most chondrule bulk compositions occupy the quadrangle Fo–En–Fs_{40}–Fa_{40}, only few plot beyond pyroxene-normative compositions, while SRCs extend the chondrule field to much more SiO_2-rich compositions, located within the triangle En–Fs_{40}–SiO_2.

The plot suggests that chondrules are mechanical mixtures of olivine-, pyroxene- and some Ca, Al-rich phases that may have formed during condensation in the solar nebula—a scenario that has been suggested earlier for the formation of OC-chondrules by Grossman and Wasson (1982, 1983). During equilibrium condensation Ca, Al-rich minerals, olivine, metal, and pyroxene condense from a gas with solar composition. Thermodynamic calculations (e.g., Ebel and Grossman, 2000) show that the SiO_2 end member is not a product of equilibrium condensation, because a solar Mg/Si-ratio of 1.07, implying approximately the same number of Mg and Si atoms (e.g., Palme and Jones, 2003) is not sufficient to condense SiO_2. Indeed, free silica is not observed in type I and II chondrules. Petaev and Wood (1998) suggested deviations from the equilibrium condensation sequence may have occurred. Either temperature decreased faster than equilibrium between gas and solids was established or early condensed crystals were removed from equilibrium. In their calculations, Petaev and Wood (1998) introduced a parameter "ξ" which they call "isolation degree". This is the percentage of solid material that is removed from equilibrium with the gas phase at any given temperature. Petaev and Wood (1998) found that as little as 0.47% isolation is sufficient to lead to condensation of SiO_2 at 10 Pa and 1215 K. This opens up the possibility that SRC precursors—as other chondrule precursors—may originate from condensation. In this view, SRCs are mixtures of condensed SiO_2 and some other minor components like, e.g., pyroxene, olivine or CAI material. Thus, the SiO_2 phases would have formed by fractional condensation.

Before further discussing fractional condensation as possible SiO_2-enrichment mechanism, we will describe three other possibilities for SRC production and explain why we believe that they are unlikely. These possibilities were briefly mentioned in the introduction: (1) RedOx-processes on a parent body, (2) fragments of SiO_2-rich chondrule mesostasis and finally (3) fractional crystallization, which we will discuss in more detail.

(1) Examples of the first possibility, the reduction of FeO-rich pyroxene to metallic Fe and SiO_2, are found in eucrites, the Camel Donga meteorite is a particularly good example (Palme et al., 1988). This possibility can be excluded for SRCs, because their parageneses do not contain metal. In addition, reduction does not change the bulk Mg/Si-ratio, which is also required.
(2) The second possibility—SRCs are recycled mesostasis fragments—can also be discarded. Chondrules contain high concentrations of SiO_2 in their mesostasis due to crystallization of the mafic phases olivine and pyroxene, but also—for the same reason—mesostasis has high concentrations of refractory elements like CaO, Al_2O_3 and REE. SRCs by definition do have high concentrations of SiO_2, but the contents of

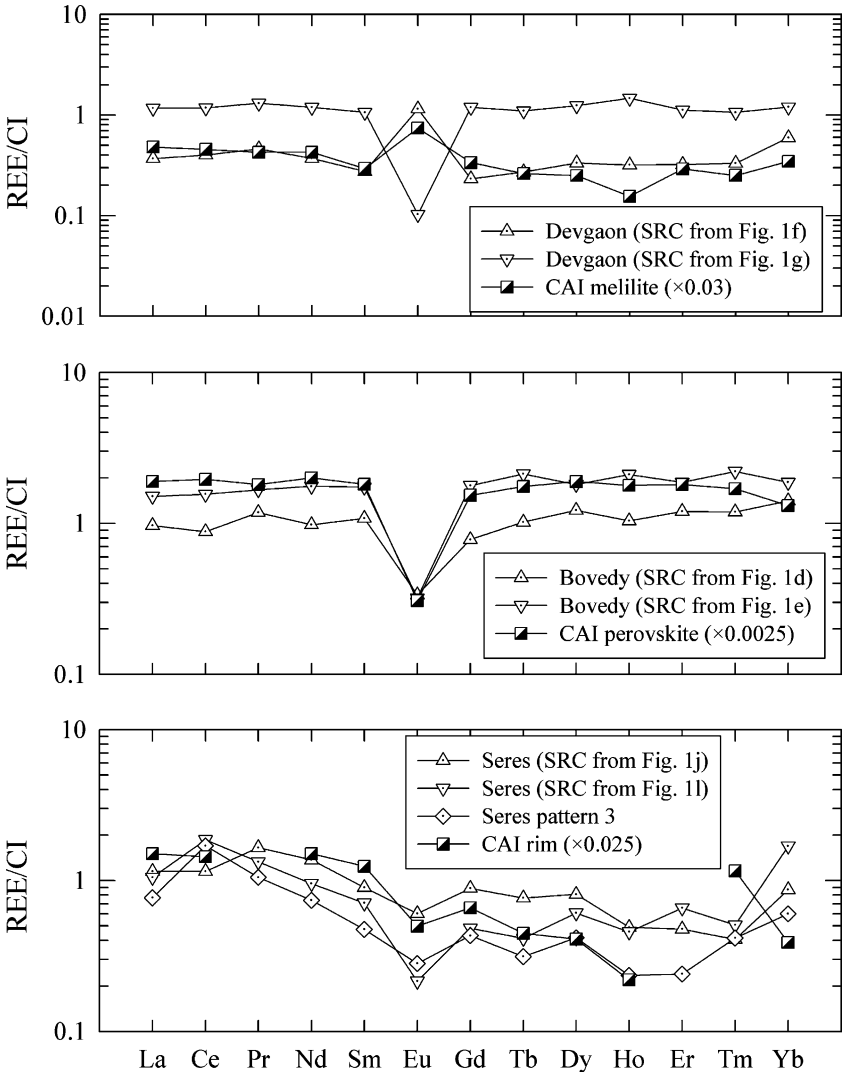

Fig. 2. Selected REE/CI-patterns for pyroxenes from different SRCs of the OCs Devgaon, Bovedy, and Seres. Patterns are usually flat and absolute concentrations are low. Additional REE-patterns are from various CAI-materials. The SRC REE-pattern may be explained by an admixture of traces of CAI material to the SRCs. The low CAI REE-concentrations are achieved by admixing 3% melilite to the Devgaon SRCs, 0.25% perovskite to the Bovedy SRCs and 2.5% CAI rim material to the Seres SRCs. (Data taken from Brearley and Jones, 1998 and references therein (melilite from Vigarano and perovskite from Efremovka) and Wark and Boynton (2001) (Allende CAI rim)). The Seres SRC from which pattern 3 was obtained is not shown in Fig. 1.

refractory elements are low, mostly subchondritic. Fig. 5 shows this difference between chondrule mesostases and SRCs for CaO and Al_2O_3. The REE in chondrule mesostases have between 4 and 20 times the CI-concentration (Alexander, 1994), in contrast the SRCs have only ~0.1–1 times the CI-concentrations.

(3) Fractional crystallization as the third possibility is favoured by Ruzicka et al. (1995) for the Bo-1 clast in Bovedy and by Bridges et al. (1995) for eight "CB"-clasts in Parnallee. Both authors suggest that silica-bearing objects in other meteorites may also have formed by magmatic processes. Fig. 4 contains compositional data of magmatic rocks from the Earth, Vesta (eucrites) and the results of model calculations of fractional crystallization (using MELTS). The calculated compositions (Fig. 4, dotted line) represent the evolution of a melt resulting from fractional crystallization of a metal free H-chondrite (see above). The trend is qualitatively similar to the trend defined by terrestrial rocks. The difference between the two trends reflects different starting compositions. The data points for eucrites coincide with the composition of terrestrial tholeiitic-basalts (the corresponding data point is hidden under the eucrite data points). An igneous clast described by Bischoff et al. (1993) in the Adzhi Bogdo meteorite (LL3-6) has a granitoidal paragenesis and defines a trend comparable to the trends seen in terrestrial rocks and calculated from MELTS (Fig. 4). In contrast, none of the Bo-1- and CB-clasts or the SRCs plots on the line defined by magmatic trends, nor do they define their own trend. To the contrary, they extend the mixing lines defined by all other chondrules. Plots of CaO and Al_2O_3 versus SiO_2 (Harker-diagrams, Fig. 6) sup-

Table 4
Trace- and RE-element concentrations in SRCs from different ordinary chondrites measured in this study (all data in ppb)

	Devgaon												
	f	f	g	h									
La	87	94	<d.l.	201	112	41	277	51	87	25	173	116	<d.l.
Ce	249	309	35	496	496	92	732	132	234	62	852	659	170
Pr	42	43	<d.l.	92	60	15	118	25	35	<d.l.	94	80	17
Nd	172	170	16	424	199	66	552	125	174	41	323	214	34
Sm	40	62	<d.l.	127	37	<d.l.	153	44	71	<d.l.	104	57	<d.l.
Eu	63	51	<d.l.	30	21	<d.l.	<d.l.	24	47	19	26	16	<d.l.
Gd	46	44	<d.l.	160	<d.l.	<d.l.	236	23	57	23	55	29	19
Tb	<d.l.	<d.l.	<d.l.	30	<d.l.	<d.l.	39	<d.l.	<d.l.	<d.l.	<d.l.	<d.l.	<d.l.
Dy	82	79	24	250	39	34	304	18	103	26	79	26	18
Ho	18	23	<d.l.	54	<d.l.	<d.l.	81	<d.l.	21	<d.l.	<d.l.	<d.l.	<d.l.
Er	52	58	<d.l.	166	23	<d.l.	182	<d.l.	72	21	41	<d.l.	<d.l.
Tm	<d.l.	<d.l.	<d.l.	18	<d.l.	<d.l.	23	<d.l.	<d.l.	<d.l.	<d.l.	<d.l.	<d.l.
Yb	99	67	41	151	32	36	198	16	128	<d I	53	83	18
Eu/Eu*	4.54	2.84	2.42	0.66	2.94	0.52	0.09	2.11	2.21	5.51	0.96	1.09	—

	Seres												Bovedy			
	i	i	j	k	k	l	l	m					d	d	e	e
La	138	47	25	164	163	247	181	338	574	272	198	227	207	145	228	356
Ce	438	108	155	376	384	1150	1050	841	1160	714	543	500	620	358	545	966
Pr	77	19	30	43	34	120	95	102	143	148	77	63	87	64	106	150
Nd	260	91	36	207	146	442	342	635	575	636	234	260	438	301	453	813
Sm	102	22	32	68	36	102	68	226	76	130	78	71	131	89	155	250
Eu	21	16	<d.l.	17	<d.l.	<d.l.	15	136	47	33	17	22	58	57	18	18
Gd	127	48	48	83	58	96	86	359	63	176	74	87	150	147	155	355
Tb	26	<d.l.	<d.l.	<d.l.	<d.l.	<d.l.	<d.l.	57	18	27	18	18	23	35	36	75
Dy	168	57	53	112	81	150	103	364	90	199	140	137	249	210	301	444
Ho	37	18	17	25	<d.l.	25	<d.l.	83	16	27	38	25	43	50	57	117
Er	162	26	51	80	71	107	39	245	76	77	127	116	154	148	194	304
Tm	42	<d.l.	<d.l.	17	<d.l.	<d.l.	<d.l.	46	<d.l.	<d.l.	21	23	29	23	26	49
Yb	307	128	85	168	135	281	100	265	162	144	269	198	236	199	233	310
Eu/Eu*	0.56	1.46	—	0.71	0.37	0.36	0.62	1.48	2.03	0.68	0.67	0.85	1.27	1.53	0.36	0.18

Eu/Eu* is the CI-normalized Eu-concentration of the individual element, divided by the CI-normalized average concentration of the Eu neighbouring elements Sm and Gd. The letters refer to the corresponding images in Fig. 1. d.l., detection limit.

port these findings: the magmatic trends defined by terrestrial rocks, eucrites or the granitoidal clast cannot explain the compositions of SRCs or the Bo-1-/CB-clasts. Eucrites, terrestrial rocks, and the granitoidal clast have high CaO- and Al_2O_3-concentrations, in addition terrestrial rocks and the Adzhi Bogdo clast have fractionated Ca/Al-ratios, with low Ca- and high Al-concentrations, contrary to what is seen in SRCs and the Parnallee clast (Fig. 6). The MELTS calculation also produces residual melts with high CaO- and Al_2O_3-concentrations, although CaO and Al_2O_3 are not fractionated. In contrast, the SRCs and the Bo-1-/CB-clasts have very low CaO- and Al_2O_3-concentrations and apparently extend the trends defined by bulk chondrules to higher SiO_2 and lower CaO and Al_2O_3, respectively. Some SRCs from the Seres meteorite have low CaO/Al_2O_3-ratios, probably the result of the presence of spinel in these SRCs. Thus, the major elements in SRCs and the Bo-1-/CB-clasts do not support a magmatic origin.

The CI-normalized patterns of REE as well as their absolute contents provide additional evidence against a magmatic origin. Low Ca-pyroxenes prefer heavy REE (HREE) over light REE (LREE) (Table 5). The SRC pyroxenes have essentially unfractionated REE-patterns, some have a positive and some a negative Eu-anomaly (Table 4), and moreover, a few pyroxenes show a slight enrichment of LREE over HREE (Fig. 2). During magmatic crystallization, pyroxenes often develop a small negative Eu-anomaly, as simultaneous crystallization of plagioclase removes Eu^{2+} from the melt. A positive Eu-anomaly in pyroxenes could develop by crystallizing from a plagioclase-enriched source. However, plagioclase preferentially incorporates LREE. If the positive/negative Eu-anomalies in SRC-pyroxenes would be the result of plagioclase crystallization, then the SRC-pyroxenes should have a pronounced LREE-depletion, which is not observed. Besides, plagioclase was never found in SRCs, except in a single case, where traces of plagioclase are a component of the mesostasis (Fig. 1a). The absence of plagioclase or any

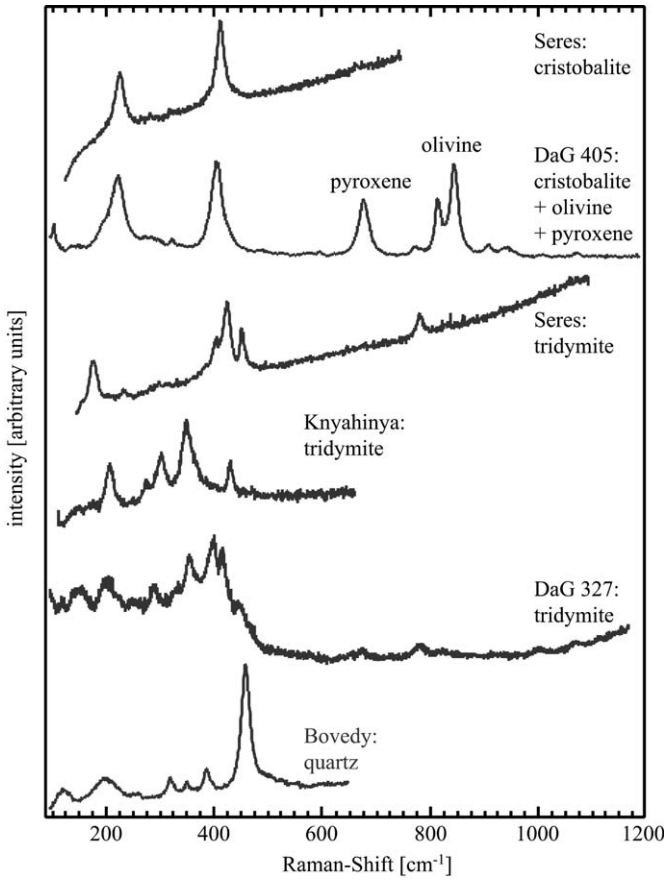

Fig. 3. Examples of micro-Raman spectra of the silica-polymorphs found in our samples. Spectra are from various meteorites, because not all meteorites studied contain the complete silica-polymorph suite we found. One spectrum has no equivalent in the literature (see text).

other possible sink for Eu contradicts the magmatic origin hypothesis of SRC formation.

The absolute concentrations of REE in SRC components is also incompatible with a magmatic origin of SRCs. Formation of SiO_2-rich lithologies from a chondritic starting material requires extensive crystallization of olivine and pyroxene. Crystallization of olivine will uniformly enrich REE in the residual melt, as olivine/melt partition coefficients are extremely low (Table 5). As the SRC pyroxenes have similar or even lower REE-concentrations down to ~0.1 times CI than those of low Ca-pyroxenes in ordinary chondrites (e.g., Curtis and Schmitt, 1979) the SRC-pyroxenes cannot have crystallized from a system enriched in REE relative to chondrites. Thus, neither the flat patterns nor the low abundance of REE in SRCs are consistent with crystallization of the pyroxenes from a liquid formed by igneous fractionation of a chondritic source.

The REE-patterns of the SRC pyroxenes instead resemble bulk chondrule REE-patterns. Flat patterns are typical of type I and II chondrules (e.g., Rubin and Wasson, 1987; Palme et al., 1992) and are generally interpreted as reflecting condensation. Nearly flat REE-patterns were also found in SRCs of CH-chondrites (Hezel et al., 2004a). The spread in La/Yb-ratios of individual SRCs in the analyzed OCs from 0.16 to 2.5 is within the normal range for bulk chondrules. For example, Rubin and Wasson (1987) found La/Yb-ratios between 0.58 and 2.49 times the CI-ratio in Allende chondrules and Palme et al. (1992) reported a spread of La/Yb-ratios from 0.88 to 1.22 times the CI-ratio in chondrules of the ordinary chondrite Y-790986. The La/Yb-ratio of the CB8 Parnallee clast studied by Bridges et al. (1995) is 2.25. Although this is somewhat elevated, it is also still within the range of type I and II chondrules.

The variability in REE-patterns with positive/negative Eu-anomalies of SRC pyroxenes may indicate the admixture of a small amount (few percent) of a refractory component, such as, for example, Ca–Al-rich inclusions (CAIs). The incorporation of refractory material to chondrules was earlier suggested by Grossman and Wasson (1982, 1983) and recently by Pack et al. (submitted to GCA). CAIs are variable in their REE-patterns (e.g., MacPherson et al., 1988; Wark and Boynton, 2001) and small fragments could deliver the REE-patterns found in SRC pyroxenes (Fig. 2).

It was shown above that the major element compositions in the CB-clasts are inconsistent with igneous fractionation. Therefore the magmatic origin proposed by Bridges et al. (1995) for these clasts requires additional disequilibrium processes. In the Bridges et al. (1995) model several steps are required to produce a composition roughly matching that of the clasts (“Bridges calc.” in Figs. 4 and 6). In the first step, Bridges et al. (1995) remove alkali elements by evaporation, then metal is drained away and finally 60–70% of an olivine fraction with a constant forsterite content of 81% is removed. The olivine removal procedure applied by Bridges et al. (1995) is completely arbitrary and is not supported by the results of experimental petrology: The olivine-pyroxene field boundary is a reaction curve at high Mg/Fe-ratios, but shifts to a cotectic line with decreasing Mg/Fe-ratios (Morse, 1980). The resulting melt would in the first case evolve to the eutectic by fractional crystallization or to the peritectic by equilibrium crystallization (Hewins and Newsom, 1988 and references therein). In case of the cotectic line, the melt would end in the eutectic independent whether fractional or equilibrium crystallization occurred. In no case could crystallization of a molten chondritic source lead to higher SiO_2-concentrations than that defined by the eutectic point of the system, which is with ~62 wt% SiO_2 too low for the CB-clasts. Another requirement would be that all crystallized olivine is in equilibrium with the melt at the time of removal, but is then instantaneously fractionated without any further reactions with the remaining melt. Thus the olivine subtraction procedure applied by Bridges et al. (1995) has no physical significance. We therefore disagree with the interpretation of Bridges et al. (1995) and suggest that these clasts or their precursors cannot have formed by magmatic processes. An origin by fractional condensation and later mixing with pyroxene and/or olivine is more likely.

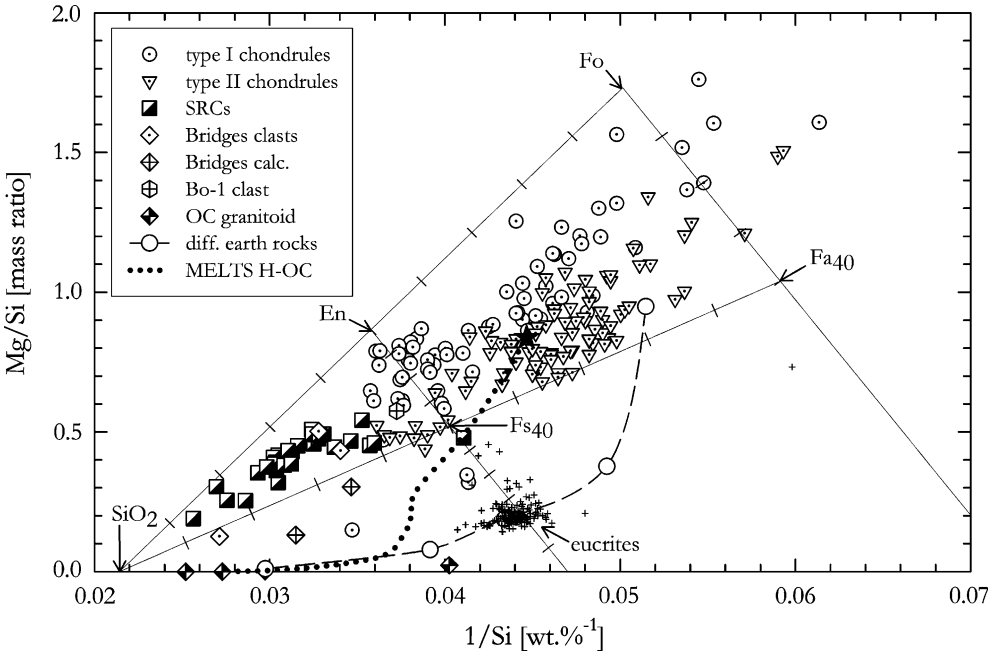

Fig. 4. The diagram shows bulk chondrule- and SRC-compositions in OCs. Fo, forsterite; En, enstatite; Fa, fayalite; and Fs, ferrosilite. The four straight lines are scaled mixing lines between Fo-SiO_2, Fo–Fa, Fa_{40}–SiO_2 and En–Fs, respectively. "Bridges clasts" are the three clasts from Parnallee (taken from Bridges et al., 1995). A clast from Bovedy is indicated Bo-1 (Ruzicka et al., 1995). "Bridges calc." are calculations from Bridges et al. (1995) (see text). "OC granitoid" indicate a granitoidal clast (Bischoff et al., 1993) in Adzhi Bogdo. The starting composition for the MELTS fractional crystallization sequence is indicated by the star (Mason, 1965). Terrestrial data ("diff. earth rocks") are in order of increasing SiO_2 (=decreasing 1/Si): komatiitic peridotite–basanite–tholeiitic basalt–andesite–granite (taken from Hughes (1982)). Bulk chondrule data are from: Dodd (1978); citeyearbib36; Grossman and Wasson (1983); Olsen (1983); Sears et al. (1984); Rubin and Pernicka (1989); Jones (1990, 1994, 1996); McCoy et al. (1991); Matsunami et al. (1993); Bridges et al. (1995); Ruzicka et al. (1995); Huang et al. (1996); Tachibana et al. (2003); Hezel et al. (2004a).

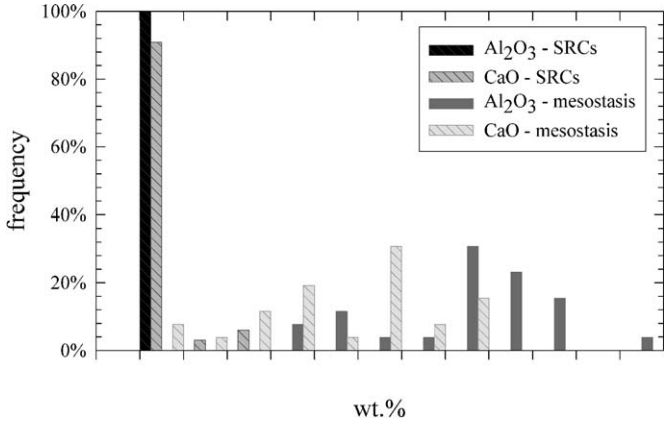

Fig. 5. The histogram shows the difference between CaO- and Al_2O_3-concentrations in SRCs and chondrule mesostases. SRCs contain much less CaO and Al_2O_3 than chondrule mesostases. (Brearley and Jones, 1998 and references therein.)

As pointed out before, there are reports of clasts of clearly igneous origin, like the Adzhi Bogdo granitoid clast, described by Bischoff et al. (1993). This clast plots at compositions expected for differentiated rocks ("OC granitoid" in Figs. 4 and 6). Also, the clast in Bovedy described in detail by Ruzicka et al. (1995), is presumably of igneous origin ("Bo-1 clast" in Figs. 4 and 6). The comparatively low content of SiO_2 (57.5%) distinguishes this clast from the more siliceous lithologies studied here. Igneous clasts like those found in Bovedy or in Adzhi Bogdo are exceptions. Most of the SiO_2-rich chondrules or fragments are of non-magmatic origin, they are mechanical mixtures of components that most likely formed by fractional condensation.

Some SRCs have parageneses deviating from those typical of SRCs and require further study. In this study, two different parageneses were encountered:

(1) SRCs with pyroxene + SiO_2 ± olivine ± spinel in Seres: The spinel observed in some of these SRCs may reflect the admixture of a Cr-rich component that condensed at comparatively low temperatures. The olivine could have crystallized from a SiO_2-rich chondrule melt, according to the SiO_2–MgO–FeO ternary. After crystallization of quartz, pyroxene and Fe-rich olivine will finally crystallize (Bowen and Schairer, 1935). This sequence corresponds to the radial zoning of objects described above with silica in the core, surrounded by a layer of pyroxene and an outer olivine layer. The olivine has moderate FeO-contents, which are far too low to fit into the sequence described above. But as Seres is of petrologic type 4, the olivine may have lost FeO during thermal parent body metamorphism. A secondary, e.g., metamorphic reaction on the parent body producing olivine does not exist. Krot and

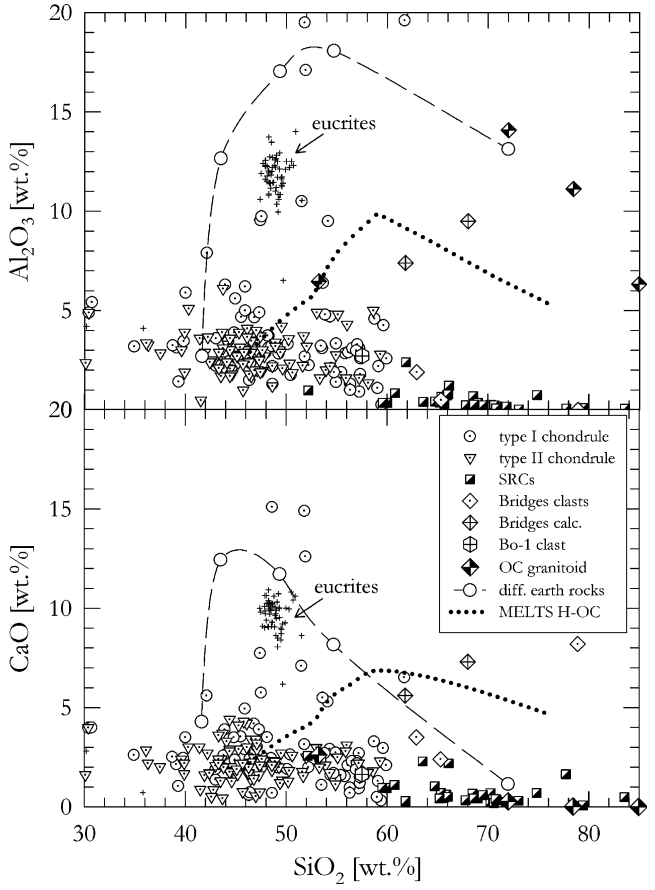

Fig. 6. Harker-diagrams for CaO and Al_2O_3 versus SiO_2. The fractionation between CaO and Al_2O_3 in magmatic systems (e.g., differentiated earth rocks, eucrites) is clearly visible, but absent in bulk chondrules, SRCs and the Parnallee clasts (see text). Symbols are similar to those in Fig. 4.

Table 5
Mineral/melt partition coefficients for different minerals

Element	ol	Low-Ca px	pl
Ce	0.00007	0.0017	0.030
Gd	0.0010	0.021	0.003
Yb	0.0194	0.087	0.007

Data from: ol, McKay (1986); low-Ca px, McKay et al. (1991); and pl, Phinney and Morrison (1990).

Wasson (1994) describe a possible hydrothermal reaction, which produces fayalite from silica and metal, but the resulting textures are very different from those of SRCs described here.

(2) Objects like the one in DaG 405 with the paragenesis SiO_2 + olivine: This object is not really a SRC (bulk SiO_2: 52.14 wt%) and can be explained as the product of rapid quenching with olivine on the liquidus. We assume that in this case the peritectic reaction olivine + SiO_2 = pyroxene is inhibited due to kinetics (Kirkpatrick et al., 1983), which results in the paragenesis olivine–SiO_2.

5. Model of SRC formation

Bulk compositions of chondrules are best explained by mechanical mixing of olivine, pyroxene, a refractory component, and an SiO_2-rich component. As there is no evidence in the bulk chemical composition of chondrules for igneous fractionation, we assume that their precursors were produced by condensation processes in the solar nebula. A similar model was proposed by Grossman and Wasson (1982, 1983), except for the SiO_2-rich component that we have added in order to explain the SRCs. As SiO_2-phases do not normally condense from a gas of solar composition, we assume that SiO_2-phases formed by fractional condensation.

In detail, we propose a two stage model for the formation of SRCs in OCs: (1) fractional condensation allows condensation of an SiO_2 phase (Petaev and Wood, 1998). The reason is probably kinetics: The first major phase to condense is olivine. Olivine reacts with nebular SiO gas producing pyroxene, according to the reaction: olivine + SiO + 1/2 O_2 = pyroxene. This reaction was successfully reproduced in the laboratory by Tissandier et al. (2002). Thereby olivine will be covered by a layer of pyroxene, which prevents further reaction of olivine and the gas. On further cooling an SiO_2-phase will condense. SRCs therefore should provide information about precursor formation predating chondrule formation. (2) In the second step these SiO_2-rich precursors were reheated—probably during the general chondrule-forming process—to minimum temperatures of 1140 K, the lower stability of tridymite, which is the most abundant silica-polymorph in SRCs. Occasionally, temperatures were above 1743 K, the low temperature stability of cristobalite. In case of one SRC in Devgaon (Fig. 1f), the temperature must have exceeded 1968 K, the temperature at which the liquid immiscibility gap opens in the system MgO–FeO–SiO_2. Quartz most probably formed from high-temperature polymorph transitions, as it is sometimes associated with tridymite and/or cristobalite. To preserve the high-temperature polymorphs, SRCs had to cool rapidly—as is generally assumed after the chondrule-forming process. A similar model was recently described for the formation of SRCs in CH-chondrites (Fig. 11 in Hezel et al., 2003). A similar scenario for the formation of silica igneous rims around chondrules in CR-chondrites has been recently suggested by Krot et al. (2004). We conclude that SRCs are normal chondrules with just very SiO_2-rich bulk compositions. Hence, if the suffix "A" in chondrule classifications stands for "olivine-rich" and "B" for "pyroxene-rich", the suffix "C" should then be used to characterize silica-rich chondrules (>65 wt% SiO_2).

The occurrence of SRCs is not surprising. It was recognized earlier by Grossman and Wasson (1982, 1983) that chondrule bulk compositions are quite variable in a given meteorite group, although the bulk compositions of group members is always the same. Chondrules with high olivine-contents must be balanced by chondrules containing pre-

dominantly pyroxene and/or silica. These requirements are consistent with fractional condensation of chondrule precursors in a separate compartment for each individual chondrite group. Fractional condensation might also be in agreement with recent results of Mostefaoui et al. (2002); Tachibana et al. (2003); Tomomura et al. (2004) and Bizzarro et al. (2004), who found (1) that chondrules formed over a time period of approximately 1–1.5 Ma and (2) that chondrules with high Si/Mg-ratios are about 1 Ma younger than chondrules with low Si/Mg-ratios.

We do not maintain here that individual chondrules must have condensed from the solar nebula, but we believe that the elemental trend seen in bulk chondrule compositions (Fig. 4) was established by mixing of components formed by condensation processes. Evaporation, recondensation, and mixing of chondrule melts may well have occurred, but partial melting and/or fractional crystallization processes were unimportant for establishing bulk chondrule compositions.

Our suggested scenario of SRC formation may also help to understand the recent discovery of SiO_2 in protosolar disks around young stellar objects (YSO), e.g., around the low mass T Tauri star HEN 3-600 A, in which—beside olivine and pyroxene—silica was detected (Honda et al., 2003). Although the Si/Mg-ratio of this star is not known (Honda, private communication) it is likely that this ratio is similar to the solar ratio, as all stars in our vicinity have Si/Mg-ratios between ~0.7 and ~1.7 and only 10% have Si/Mg-ratios <1, within most of these 10% still have ratios close to 1 (e.g., Ferrarotti and Gail, 2001).

Acknowledgments

We thank Gero Kurat, Addi Bischoff, Andreas Pack, and especially John Bridges—because we disagree with his interpretations concerning the Parnallee clasts—for providing samples. We thank Peter Hoppe and Elmar Gröner for the possibility and the help measuring the REE in Mainz. Pedro Garcia is thanked for preparing first class thin sections. Thanks are also due to Wolfgang Hofmeister for giving us the opportunity to use the Raman microprobe system at Mainz. This project was funded by DFG grant PA 346/32-1. Special thanks from D. Hezel to Thorbjörn Schönbeck for fruitful discussions. The authors are grateful to G. Libourel and J. Bridges for their thorough and helpful reviews and to the GCA associate editor S. Russell for her work and helpful comments.

Associate editor: Sara S. Russell

References

Alexander, C.M.O'D., 1994. Trace element distributions within ordinary chondrite chondrules: implications for chondrule formation conditions and precursors. *Geochim. Cosmochim. Acta* **58**, 3451–3467.

Binns, R.A., 1967. Farmington meteorite: cristobalite xenoliths and blackening. *Science* **156**, 1222–1226.

Bischoff, A., Geiger, T., Palme, H., Spettel, B., Schultz, L., Scherer, P., Schlüter, J., Lkhamsuren, J., 1993. Mineralogy, chemistry, and noble gas contents of Adzhi-Bogdo—an LL3-6 chondritic breccia with L-chondritic and granitoidal clasts. *Meteoritics* **28**, 570–578.

Bizzarro, M., Baker, J.A., Haack, H., 2004. Mg isotope evidence for contemporaneous formation of chondrules and refractory inclusions. *Nature* **431**, 275–278.

Bowen, N.L., Schairer, J.F., 1935. The system MgO–FeO–SiO_2. *Am. J. Sci.* **29**, 151–217.

Brandstätter, F., Kurat, G., 1985. On the occurrence of silica in ordinary chondrites (abstr.). *Meteoritics* **20** (Suppl.), 615.

Brearley, A.J., Jones, R.H., 1998. Chondritic meteorites. In: Papike, J.J. (Ed.), *Reviews in Mineralogy: Planetary Materials*, 36. Mineralogical Society of America, Washington, DC, p. 398.

Bridges, J.C., Franchi, I.A., Hutchinson, R., Morse, A.D., Long, J.V.P., Pillinger, C.T., 1995. Cristobalite-and tridymite-bearing clasts in Parnallee (LL3) and Farmington (L5). *Meteoritics* **30**, 715–727.

Brigham, C.A., Murrell, M.T., Yabuki, H., Ouyang, Z., El Goresy, A., 1986. Silica-bearing chondrules and clasts in ordinary chondrites. *Geochim. Cosmochim. Acta* **50**, 1655–1666.

Christophe-Michel-Levy, M., Curien, H., 1965. Etude à la microsonde électronique d'un chondre d'ol et d'un fragment riche en critobalite de la météorite de Nadiabondi. *B Soc. Fr Mineral Cr* **88**, 122–125.

Curtis, D.B., Schmitt, R.A., 1979. The petrogenesis of L-6 chondrites: insights from the chemistry of minerals. *Geochim. Cosmochim. Acta* **43**, 1091–1103.

Dodd, R.T., van Schmus, W.R., Marvin, U.B., 1965. Merrihueite, a new alkali-ferromagnesian silicate from the Mezö-Madaras chondrite. *Science* **149**, 972–974.

Dodd, R.T., van Schmus, W.R., Marvin, U.B., 1966. Significance of iron-rich silicates in the Mezö-Madaras chondrite. *Am. Mineral.* **51**, 1177–1191.

Dodd, 1978. The composition and origin of large microporphyritic chondrules in the Manych L-3 chondrite. *Earth Planet. Sci. Lett.* **39**, 52–66.

Ebel, D.S., Grossman, L., 2000. Condensation in dust-enriched systems. *Geochim. Cosmochim. Acta* **64**, 339–366.

Etchepare, J., Merian, M., Smetankine, L., 1974. Vibrational normal modes of SiO_2. I. α- and β-quartz. *J. Chem. Phys.* **60**, 1873–1876.

Etchepare, J., Merian, M., Kaplan, P., 1978. Vibrational normal modes of SiO_2. II. cristobalite and tridymite. *J. Chem. Phys.* **68**, 1531–1537.

Ferrarotti, A.S., Gail, H.-P., 2001. Mineral formation in stellar winds II. Effects of Mg/Si abundance variations on dust composition in AGB stars. *Astron. Astrophys.* **371**, 133–151.

Fredriksson, K., Wlotzka, F., 1985. Morro do Rocio: an unequilibrated H5 chondrite. *Meteoritics* **20**, 467–478.

Fujimaki H., Matsu-Ura M., Aoki K., Sunagawa I., 1981. Ferro-pseudobrookite-silica mineral-albite-chondrule in the ALHA 77015 chondrite (L3). *Proc. NIPR Symp. Anatact. Meteor.* **6**, 119–123.

Grossman, J.N., Wasson, J.T., 1982. Evidence for primitive nebular components in chondrules from the Chainpur chondrite. *Geochim. Cosmochim. Acta* **46**, 1081–1099.

Grossman, J.N., Wasson, J.T., 1983. Refractory precursor components of Semarkona chondrules and the fractionation of refractory elements among chondrites. *Geochim. Cosmochim. Acta* **47**, 759–771.

Ghiorso, M.S., Sack, R.O., 1995. Chemical mass transfer in magmatic processes. IV. a revised and internally consistent thermodynamic model for the interpolation and extrapolation of liquid–solid equilibria in magmatic systems at elevated temperatures and pressures. *Contrib. Mineral. Petr.* **119**, 197–212.

Hamilton, P.J., Evensen, N.M., O'Nions, R.K., 1979. Chronology and chemistry of Parnallee (LL-3) chondrules. *Lunar and Planetary Science X*. Lunar and Planetary Institute, Houston.

Hewins, R.H., Newsom, H.E., 1988. Igneous activity in the early solar system. *Meteorites and the Early Solar System*, pp. 73–101.

Hezel, D.C., 2003. Die Bildung SiO_2-reicher Phasen im frühen Sonnensystem. PhD-thesis, Cologne, 131 p.

Hezel, D.C., Palme, H., Brenker, F.E., Nasdala, L., 2003. Evidence for fractional condensation and reprocessing at high temperatures in CH-chondrites. *Meteorit. Planet. Sci.* **38**, 1199–1216.

Hezel, D.C., Palme, H., Brenker, F.E., 2004a. Composition and origin of SiO_2-rich objects in carbonaceaous and ordinary chondrites. *Lunar and Planetary Science XXXV*. Lunar and Planetary Institute, Houston.

Hezel, D.C., Palme, H., Brenker, F.E., 2004b. Formation of SiO_2-rich chondrules by fractional condensation. Chondrites and the protoplanetary disk workshop. #9095 (abstr.).

Honda, M., Kataza, H., Okamoto, Y.K., Miyata, T., Yamashita, T., Sako, S., Takubo, S., Onaka, T., 2003. Detection of crystalline silicates around the T Tauri star Hen 3-600A. *Astrophys J.* **585**, L59–L63.

Huang, S., Lu, J., Prinz, M., Weisberg, M.K., Benoit, P.H., Sears, D.W.G., 1996. Chondrules: their diversity and the role of open-system processes during their formation. *Icarus* **122**, 316–346.

Hughes, C.J., 1982. Igneous petrology. *Series Developments in Petrology* **7**, 551 p.

Jones, R.H., 1990. Petrology and mineralogy of Type II, FeO-rich chondrules in Semarkona (LL3.0)—origin by closed-system fractional crystallization, with evidence for supercooling. *Geochim. Cosmochim. Acta* **54**, 1785–1802.

Jones, R.H., 1994. Petrology of FeO-poor, porphyritic pyroxene chondrules in the Semarkona chondrite. *Geochim. Cosmochim. Acta* **58**, 5325–5340.

Jones, R.H., 1996. FeO-rich, porphyritic pyroxene chondrules in unequilibrated ordinary chondrites. *Geochim. Cosmochim. Acta* **60**, 3115–3117.

Kimura, M., Yagi, K., 1980. Crystallization of chondrules in ordinary chondrites. *Geochim. Cosmochim. Acta* **44**, 589–595.

Kirkpatrick, R.J., Reck, B.H., Pelly, I.Z., Kuo, L.-C., 1983. Programmed cooling experiments in the system MgO–SiO_2: kinetics of a peritectic reaction. *Am. Mineral.* **68**, 1095–1101.

Klöck, W., Thomas, K.L., McKay, D.S., Palme, H., 1989. Unusual ol and pyroxene composition in interplanetary dust and unequilibrated ordinary chondrites. *Nature* **339**, 126–128.

Kretz, R., 1983. Symbols for rock-forming minerals. *Am. Mineral.* **68**, 277–279.

Kring, D.A., Cohen, B.A., Swindle, T.D., Hill, D.H., 2000. Regolith breccia (Ourique) with impact melt clasts and other debris from an H-chondrite parent body. *Lunar and Planetary Science XXXI*. Lunar and Planetary Institute, Houston.

Krot, A.N., Wasson, J.T., 1994. Silica-merrihueite/roedderite-bearing chondrules and clasts in ordinary chondrites: new occurrences and possible origin. *Meteoritics* **29**, 707–718.

Krot, A.N., Libourel, G., Goodrich, C., Petaev, M.I., 2004. Silica-igneous rims around magnesian chondrules in CR carbonaceous chondrites: evidence for fractional condensation during chondrule formation. *Meteorit. Planet. Sci.* **39**, 1931–1955.

Lauretta, D.S., Buseck, P.R., 2003. Opaque minerals in chondrules and fine-grained chondrule rims in the Bishunpur (LL3.1) chondrite. *Meteorit. Planet. Sci.* **38**, 59–80.

Mason, B., 1965. The chemical composition of olivine-bronzite and olivine hypersthene chondrites. *Amer. Mus. Novitates No.*, 2223.

Matsunami, S., Ninagawa, K., Nishimura, S., Kubono, N., Yamamoto, I., Kohata, M., Wada, T., Yamashita, Y., Lu, J., Sears, D.W.G., Nishimura, H., 1993. Thermoluminescence and compositional zoning in the mesostasis of a Semarkona group A1 chondrule and new insights into the chondrule-forming process. *Geochim. Cosmochim. Acta* **57**, 2101–2110.

MacPherson, G.J., Wark, D.A., Armstong, J.T., 1988. Primitive material surviving chondrites—refractory inclusions. In: Kerridge, Matthews, M.S. (Eds.), *Meteorites and the Early Solar System*. The University of Arizona Press, pp. 746–807.

McCoy, T.J., Scott, E.R.D., Jones, R.H., Keil, K., Taylor, G.J., 1991. Composition of chondrule silicates in LL3-5 chondrites and implications for their nebular history and parent body metamorphism. *Geochim. Cosmochim. Acta* **55**, 601–619.

McKay, G.A., 1986. Crystal–liquid partitioning of REE in basaltic systems: extreme fractionation of REE in olivine. *Geochim. Cosmochim. Acta* **50**, 69–79.

McKay, G.A., Wagstaff, J., Le, L., 1991. REE distribution coefficients for pigeonite: constraints on the origin of the mare basalt europium anomaly. *Lunar and Planetary Science XXI*. Lunar and Planetary Institute, Houston.

Morse, S.A., 1980. Basalts and Phase Diagrams. Springer-Verlag, New York, 493p.

Mostefaoui, S., Kita, N.T., Togashi, S., Tachibana, S., Nagahara, H., Morishita, Y., 2002. The relative formation ages of ferromagnesian chondrules inferred from their initial aluminum-26/aluminum-27 ratios. *Meteorit. Planet. Sci.* **37**, 421–438.

Murty, S.V.S., Rai, V.K., Shukla, A.D., Srinivasan, G., Shukla, P.N., Suthar, K.M., Bhandari, N., Bischoff, A., 2004. Devgaon (H3) chondrite: classification and complex cosmic ray exposure history. *Meteorit. Planet. Sci.* **39**, 387–399.

Nasdala, L., Wopenka, B., Lengauer, C.L., 2004. Discussion on: transformation of SiO_2 to the amorphous state by shearing at high pressure, by Furuichi et al. (vol. 88, pp. 926–928, 2003). *Am. Mineral.* **89**, 912–913.

Newton, J., Bischoff, A., Arden, J.W., Franchi, I.A., Geiger, T., Greshake, A., Pillinger, C.T., 1995. Acfer 094, a uniquely primitive carbonaceous chondrite from the Sahara. *Meteoritics* **30**, 47–56.

Olsen, E.J., Mayeda, T.K., Clayton, R.N., 1981. Cristobalite-pyroxene in an L6 chondrite—implications for metamorphism. *Earth Planet. Sci. Lett.* **56**, 82–88.

Olsen, E.J., 1983. SiO_2-bearing chondrules in the Murchison (C2) meteorite. In: King, E.A. (Ed.), *Chondrules and their Origins*. Lunar and Planetary Institute, Houston, pp. 223–234.

Palme, H., Wlotzka, F., Spettel, B., Dreibus, G., Weber, H., 1988. Camel Donga: a eucrite with high metal content. *Meteoritics* **23**, 49–57.

Palme, H., Spettel, B., Wänke, H., Ikeda, Y., 1992. The composition of chondrules in the H3-4 chondrite Y-790986. *Antarct. Meteorit. XVII*, 86–88.

Palme, H., Jones, A., 2003. Solar system abundances of the elements 41–62. In: Davis, A.M. (Ed.), *Meteorites, Comets and Planets*. In: Holland, H.D., Turekian, K.K. (Eds.), *Treatise on Geochemistry*, vol. 1. Elsevier-Pergamon, Oxford.

Petaev, M.I., Wood, J.A., 1998. The condensation with partial isolation (CWPI) model of condensation in the solar nebula. *Meteorit. Planet. Sci.* **33**, 1123–1137.

Phinney, W.C., Morrison, D.A., 1990. Partition coefficients for calcic plagioclase: implications for Archean anorthosites. *Geochim. Cosmochim. Acta* **54**, 1639–1654.

Planner, H.N., 1983. Phase separation on a chondrule fragment from the Piancaldoli (LL3) chondrite. In: King, E.A. (Ed.), *Chondrules and their Origins*. Lunar and Planetary Institute, Houston, pp. 235–242.

Pride, A.K.A., Dove, M.T., 1998. On the sequence of phase transitions in tridymite. *Phys. Chem. Miner.* **26**, 171–179.

Rubin, A.E., 1983. The Adhi Kot breccia and implications for the origin of chondrules and silica-rich clasts in enstatite chondrites. *Earth Planet. Sci. Lett.* **64**, 201–212.

Rubin, A.E., Wasson, J.T., 1987. Chondrules, matrix and coarse-grained chondrule rims in the Allende meteorite—origin, interrelationships, and possible precursor components. *Geochim. Cosmochim. Acta* **51**, 1923–1937.

Rubin, A.E., Pernicka, E., 1989. Chondrules in the Sharps H3 chondrite—evidence for intergroup compositional differences among ordinary chondrite chondrules. *Geochim. Cosmochim. Acta* **53**, 187–195.

Ruzicka, A., Boynton, W.V., 1992. A distinctive silica-rich, sodium-poor igneous clast in the Bovedy (L3) chondrite. *Meteoritics* **27**, 283.

Ruzicka, A., Kring, D.A., Hill, D.H., Boynton, W.V., 1993. The trace element composition of a silica-rich clast in the Bovedy (L3/4) chondrite. *Meteoritics* **28**, 426–427.

Ruzicka, A., Kring, D.A., Hill, D.H., Boynton, W.V., Clayton, R.N., Mayeda, T.K., 1995. Silica-rich orthopyroxenite in the Bovedy chondrite. *Meteoritics* **30**, 57–70.

Scott, J.F., Porto, S.P.S., 1967. Longitudinal and transversal optical lattice vibrations in quartz. *Phys. Rev.* **161**, 903–910.

Sears, D.W.G., Sparks, M.H., Rubin, A.E., 1984. Chemical and physical studies of type 3 chondrites. III chondrules from the Dhajala H3.8 chondrite. *Geochim. Cosmochim. Acta* **48**, 1189–1200.

Sharma, S.K., Mammone, J.F., Nicol, M.F., 1981. Raman investigation of ring configurations in vitreous silica. *Nature* **292**, 140–141.

Tachibana, S., Nagahara, H., Mostefaoui, S., Kita, N.T., 2003. Correlation between relative ages inferred from ^{26}Al and bulk compositions of ferromagnesian chondrules in least equilibrated ordinary chondrites. *Meteorit. Planet. Sci.* **38**, 939–962.

Tissandier, L., Libourel, G., Robert, F., 2002. Gas-melt interactions and their bearing on chondrule formation. *Meteorit. Planet. Sci.* **37**, 1377–1389.

Tomomura, S., Nagahara, H., Tachibana, S., Kita, N.T., Marishita, Y., 2004. Relationship between bulk chemical composition and formation age of chondrules in Bishunpur and Krymka. *Lunar and Planetary Science XXXV*. Lunar and Planetary Institute, Houston.

Wark, D., Boynton, W.V., 2001. The formation of rims on calcium-aluminum-rich inclusions: step I—flash heating.

Wasson, J.T., Krot, A.N., 1994. Fayalite-silica association in unequilibrated ordinary chondrites: evidence for aqueous alteration on a parent body. *Earth Planet. Sci. Lett.* **122**, 403–416.

Withers, R.L., Thompson, J.G., Xiao, Y., Kirkpatrick, R.J., 1994. An electron diffracton study of the polymorphs of SiO_2-tridymite. *Phys. Chem. Miner.* **21**, 421–433.

Wlotzka, F., Fredriksson, K., 1980. Morro do Rocio, unequilibrated H5 chondrite. *Meteoritics* **15**, 387–388.

Wood, J.A., Holmberg, B.B., 1994. Constraints placed on the chondrule-forming process by merrihueite in the Mezö-Madaras chondrite. *Icarus* **108**, 309–324.